Macromolecules

Article

pubs.acs.org/Macromolecules

Irreversible Low Critical Solution Temperature Behaviors of Thermal-responsive OEGylated Poly(L-cysteine) Containing Disulfide Bonds

Yinan Ma, Xiaohui Fu, Yong Shen, Wenxin Fu,* and Zhibo Li*

Beijing National Laboratory for Molecular Sciences (BNLMS), Institute of Chemistry, Chinese Academy of Sciences, Beijing 100190, China

Supporting Information

ABSTRACT: Three cysteine derivatives were synthesized in high yield by ligating monomethoxy oligo(ethylene glycol) (OEG) to L-cysteine thiol group using sulfenyl chlorides. These OEG groups containing di-, tri-, and tetra-EG units were linked with L-cysteine via disulfide bond. The three monomers were then converted into corresponding *N*-carboxyanhydrides (NCAs) using triphosgene in THF. Subsequent ring-opening polymerization (ROP) of disulfide bond containing NCAs gave three poly-EG_x-L-cysteine derivatives. The obtained poly-EG_x-L-cysteine with x = 3 and 4 displayed thermal-responsive behaviors in water, but the temperature-induced phase transition was found surprisingly irreversible. Such irreversible thermal-responsive behaviors were attributed to cross-linking arising from disulfide bonds exchanges. Using PEG-NH_2 as macroinitiator, we also prepared two PEG-*b*-poly-EG_x-L-cysteine diblocks, which could undergo irreversible thermal-induced sol−gel transition, which was caused by the disulfide bonds exchanging reactions. These hydrogels displayed partially shear-thinning and rapid recovery properties allowing new capabilities to construct stimuli-responsive injectable hydrogels in biomedical applications.

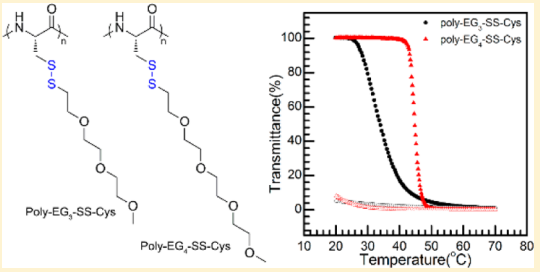

INTRODUCTION

Disulfide bonds *in vivo* are pivotal in the folding and stability of proteins, and their multifaceted roles are launched in peptide/protein drug design to stabilize secondary structures and enhance bioactivity and selectivity.[1] Depending on the different reduction−oxidation (redox) environment, disulfide bonds can be converted into different forms, such as thiol, thiosulfinate/thiosulfonate, or even sulfenic acid/sulfinic acid.[2] In biosystems, disulfide bonds are generally formed by sulfur-containing amino acid such as cysteine. The disulfide bonds, which can be formed through thiol−disulfide exchange reaction,[3] could be rearranged to form sophisticated inter- and intramolecular cross-linking structures, which are crucial for redox homeostasis in cells.[4]

Poly(L-cysteine) is a β-sheet forming hydrophobic polypeptide.[5] Owing to the low redox potential of thiol groups, it is susceptible to oxidation giving sulfoxide/sulfone or disulfide. Recently, excellent works have been reported on functionalized cysteine *N*-carboxyanhydrides (NCAs) and related poly(L-cysteine) derivatives. Kramer and Deming reported the preparation of glycosylated L-cysteine using thiol−ene click reaction, from which they constructed redox-responsive glycopolypeptides.[6] Zhong and co-workers developed vinyl sulfone-substituted L-cysteine to afford functionalized polypeptides.[7] Gupta synthesized water-soluble phosphate and phosphonate containing poly(L-cysteine)s via ROP of NCAs, mimicking natural phosphorylated proteins.[8] Dong group designed a photoresponsive *S*-(*o*-nitrobenzyl)-L-cysteine NCA and the related block copolypeptides could serve as photo-triggered drug carriers.[9] Very recently, an oligo(ethylene glycol) (OEG) functionalized poly(L-cysteine) were reported to display dual thermal- and oxidation-responsive behaviors.[10,11] Diblock copolymers composed of such OEGylated poly(L-cysteine) and poly(ethylene glycol) (PEG) could form responsive micelles, which were promising carriers for inflamed tissue targeting drug delivery.[11] Whereas, the reported functional group, e.g., saccharides, bioactive molecules, reactive precursors, were linked via thioether (−S−) or thiocarbonate (−S-C(═O)−O−) bonds with cysteine side chains.

Compared with thioether and thiocarbonate bonds, disulfide bonds show superior reactivity for cross-reaction or site-specific reactions. For example, various reduction-responsive polymers and conjugates were employed for intracellular triggered drug/gene delivery, involving disulfide linkage(s) at different sites.[12] Considering these advantages, introducing disulfide bonds into polypeptide side chains would be a promising strategy to construct interchangeable multi-responsive systems. Herein, we report the preparation of OEGylated disulfide bond-containing polypeptides based on L-cysteine (Scheme 1). The key points are the simultaneous incorporation of OEG unit and disulfide bonds to polypeptide side chains. The OEG units offer possible thermal-responsive functionality, while the disulfide groups provide a reduction-responsive switch and thiol−disulfide exchange reaction sites.

Received: May 27, 2014
Revised: June 26, 2014
Published: July 14, 2014

   dx.doi.org/10.1021/ma501104s | *Macromolecules* 2014, 47, 4684−4689

Scheme 1. Synthetic Routes toward Thermal-Responsive Polypeptides from L-Cysteine[a]

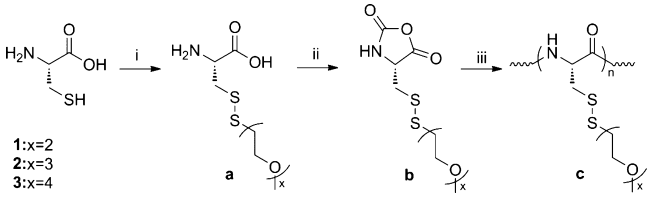

[a]Reagents and conditions: (i) OEG sulfenyl chloride (EG_x–S–Cl, x = 2, 3, 4), $NaHCO_3$, MeOH, 0 °C to room temperature, 2 h. (ii) Triphosgene, THF, 50 °C, 4 h. (iii) Hexamethyldisilazane (HMDS), THF/DMF 1:1 v/v, 25 °C, 24 h.

EXPERIMENTAL SECTION

Materials and Methods. Hexane, tetrahydrofuran (THF), and dichloromethane (DCM) were deoxygenated and dried by purging with nitrogen and passage through activated alumina columns prior to use. Ethyl acetate (EtOAc) was freshly distilled from CaH_2. *N*,*N*-Dimethylformamide (DMF) was treated with free amine scavenger (Aldrich) before passed through 4 Å molecular sieves and activated alumina column. Pyrogen free deionized water (18 MΩ·cm) was obtained from a Millipore Milli-Q Biocel A10 purification unit. Methoxypolyethylene glycol amine ($mPEG_{45}$-NH_2, M_w = 2000) was purchased from Jenkem Technology Co, Ltd. (Beijing, China). All other chemicals were purchased from commercial suppliers and used without further purification unless otherwise noted. Reaction temperatures were controlled using an IKA temperature modulator. Unless otherwise stated, reactions were performed at room temperature, ca. 20 °C. ^{1}H and ^{13}C NMR spectra were acquired on Bruker AV400FT-NMR spectrometer. Electron spray ionization tandem mass spectrometry (ESI-MS) was recorded on a Shimadzu Inc. LCMS-2010 spectrometer. All Fourier transform infrared (FTIR) spectra were performed using a Nicolet Avatar 330 FT-IR spectrometer. The solution samples were cast on KBr plates before measurement. The solid samples was milled with potassium bromide (Aldrich) at mass ratio of 1:100 and pressed into disk before FTIR measurements. Tandem gel permeation chromatography/light scattering (GPC/LS) was performed at 50 °C using an SSI pump connected to Wyatt Optilab DSP and Wyatt DAWN EOS light scattering (LS) detectors with 0.02 M LiBr in DMF as the eluent at flow rate of 1.0 mL/min. All GPC/LS samples were prepared at concentrations of 5 mg/mL. The cloud points (CPs) were measured by monitoring the transmittance of a 500 nm light beam through a quartz sample cell on a Shimadzu UV–vis spectrometer, and defined as the temperatures corresponding to 50% transmittance of aqueous solution during the heating process. Dynamic light scattering (DLS) measurements were performed using a Malvern Nanozetasizer. Circular dichroism (CD) spectra were recorded on a JASCO J-815 CD Spectropolarimeter. The solution was placed into a quartz cell with a path length of 1.0 mm with temperature controlled by a water bath, and the concentration of samples was 0.1 mg/mL. The secondary structures were analyzed on DICHROWEB using Contin-LL.[13,14] Rheology measurements were performed on a Rheometrics ARES controlled strain rheometer in cone–plate geometry with 40 mm diameter and 1° cone angle.

Synthesis of OEGylated Disulfide-Containing L-Cysteine Derivatives [EG_x-SS-Cys] (1a–3a). EG_x–SH (x = 2, 3, 4) were synthesized using oligo(ethylene glycol) monomethyl ethers according to the literature procedures.[15] A solution of EG_x-SH (30 mmol, 4.08, 5.40, and 6.73 g) in dry DCM (20 mL) was degassed via three freeze–pump–thaw cycles and kept at 0 °C in ice bath. Then sulfuryl chloride (4.45 g, 33 mmol, 1.1 equiv) was added dropwise using syringe under N_2. The reaction mixture was stirred for 3 h to obtain orange-yellow oligo(ethylene glycol) sulfenyl chloride (EG_x-S-Cl). A suspension of L-cysteine hydrochloride (4.73 g, 30 mmol) and $NaHCO_3$ (5.04 g, 60 mmol, 2.0 equiv) in methanol (100 mL) was degassed via three freeze–pump–thaw cycles before adding EG_x-S-Cl at 0 °C under N_2. After the mix was stirred for 2 h, another 100 mL of methanol was added into the suspension, and the insoluble products were removed via centrifugation. The solvent was then removed using rotavaporator. The obtained samples were washed using ether three times to give white to pale yellow solids, i.e., **1a**, **2a**, and **3a**, respectively.

*S-(2-(2-Methoxyethoxy)ethyl)thio-L-cysteine (EG_2-SS-Cys), **1a** (6.5 g, 85% Yield).* ^{1}H NMR (400 MHz, D_2O): δ 4.47–4.35 (m, 1H), 3.84 (t, 2H), 3.76–3.68 (m, 2H), 3.67–3.58 (m, 2H), 3.49–3.39 (m, 1H), 3.37 (s, 3H), 3.32–3.17 (m, 1H), 3.00 (t, 2H). ^{13}C NMR (101 MHz, D_2O): δ 171.03, 71.06, 69.33, 68.31, 58.15, 52.09, 37.03, 36.60. HRMS-ESI (m/z) [M + H]$^+$: calcd for $C_8H_{18}NO_4S_2$, 256.06722; found, 256.06718.

*S-(2-(2-(2-Methoxyethoxy)ethoxy)ethyl)thio-L-cysteine (EG_3-SS-Cys), **2a** (7.1 g, 79% Yield).* ^{1}H NMR (400 MHz, D_2O): δ 4.51–4.41 (m, 1H), 3.89–3.79 (m, 2H), 3.78–3.65 (m, 6H), 3.65–3.59 (m, 2H), 3.51–3.40 (m, 1H), 3.37 (s, 3H), 3.32–3.17 (m, 1H), 3.01 (t, 2H). ^{13}C NMR (101 MHz, D_2O): δ 170.83, 71.17, 69.66, 69.58, 69.56, 68.40, 58.24, 52.03, 37.08, 36.50. HRMS-ESI (m/z) [M + H]$^+$: calcd for $C_{10}H_{22}NO_5S_2$, 300.09330; found, 300.09339.

*S-(2-(2-(2-(2-Methoxyethoxy)ethoxy)ethoxy)ethyl)thio-L-cysteine (EG_4-SS-Cys), **3a** (7.3 g, 71% Yield).* ^{1}H NMR (400 MHz, D_2O): δ 4.51–4.44 (m, 1H), 3.88–3.79 (m, 2H), 3.77–3.63 (m, 10H), 3.63–3.57 (m, 2H), 3.49–3.39 (m, 1H), 3.36 (s, 3H), 3.32–3.21 (m, 1H), 3.00 (t, 2H). ^{13}C NMR (101 MHz, D_2O) δ 170.66, 71.15, 69.72, 69.67, 69.63, 69.57, 69.55, 68.40, 58.25, 51.89, 37.05, 36.37. HRMS-ESI (m/z) [M + H]$^+$: calcd for $C_{12}H_{26}NO_6S_2$, 344.11939; found, 344.11961.

Synthesis of NCAs [EG_x-SS-Cys NCAs] (1b-3b). **1a** (2.55 g, 10 mmol), **2a** (2.99 g, 10 mmol), or **3a** (3.24 g, 10 mmol) was dissolved in dry THF (100 mL), and triphosgene (1.16 g, 3.9 mmol, 0.39 equiv) was then charged into a 250 mL round-bottom Schlenk flask. The mixture was stirred at 50 °C under N_2 for 4 h, and the solvent was then removed under reduced pressure to give yellowish-brown oil, which was subsequently purified by flash column chromatography using EtOAc/hexane (1:1–3:1 v/v) as eluent.

*S-(2-(2-Methoxyethoxy)ethyl)thio-L-cysteine-N-carboxyanhydride (EG_2-SS-Cys NCA), **1b** (1.62 g, 58% Yield).* ^{1}H NMR (400 MHz, DMSO-d_6): δ 9.24 (s, 1H), 4.78 (m, 1H), 3.62 (t, 2H), 3.53 (dd, 2H), 3.44 (dd, 2H), 3.24 (s, 3H), 3.18 (dd, 2H), 2.96–2.87 (m, 2H). ^{13}C NMR (101 MHz, DMSO-d_6): δ 170.86, 152.43, 71.81, 69.99, 69.00, 58.68, 57.34, 40.20, 38.50. FTIR (THF): 2878, 1858, 1786, 1457, 1355, 1285, 1092, 925 cm^{-1}. Anal. Calcd for $C_9H_{15}NO_5S_2$: C, 38.42; H, 5.37; N, 4.98; S, 22.79. Found: C, 39.63; H, 5.78; N, 4.46; S, 20.34.

*S-(2-(2-(2-Methoxyethoxy)ethoxy)ethyl)thio-L-cysteine-N-carboxyanhydride (EG_3-SS-Cys NCA), **2b** (1.72 g, 53% Yield).* ^{1}H NMR (400 MHz, DMSO-d_6): δ 9.23 (br, 1H), 4.84–4.70 (m, 1H), 3.63 (t, 2H), 3.51 (dd, 6H), 3.42 (dd, 2H), 3.23 (s, 3H), 3.18 (dd, 2H), 2.96–2.86 (m, 2H). ^{13}C NMR (101 MHz, DMSO-d_6): δ 170.85, 152.41, 71.86, 70.30, 70.18, 69.01, 58.64, 57.31, 40.16, 38.45. FTIR (THF): 2877, 1856, 1785, 1455, 1353, 1286, 1097, 926 cm^{-1}. HRMS-MALDI (m/z) [M + Na]$^+$: calcd for $C_{11}H_{19}NO_6S_2Na$, 348.05460; found, 348.05462. Anal. Calcd for $C_{11}H_{19}NO_6S_2$: C, 40.60; H, 5.89; N, 4.30; S, 19.71. Found: C, 40.94; H, 6.09; N, 4.05; S, 18.57.

*S-(2-(2-(2-(2-Methoxyethoxy)ethoxy)ethoxy)ethyl)thio-L-cysteine-N-carboxyanhydride (EG_4-SS-Cys NCA), **3b** (1.85 g, 50% Yield).* ^{1}H NMR (400 MHz, DMSO-d_6): δ 9.24 (br, 1H), 4.90–4.74 (m, 1H), 3.64 (t, 2H), 3.51 (dd, 10H), 3.43 (dd, 2H), 3.24 (s, 3H), 3.21–3.16 (m, 2H), 2.97–2.81 (m, 2H). ^{13}C NMR (101 MHz, DMSO-d_6): δ 170.75, 152.32, 71.79, 70.32, 70.29, 70.24, 70.10, 68.94, 58.56, 57.25, 40.12, 38.41. FTIR (THF): 2877, 1856, 1786, 1459, 1351, 1289, 1249, 1101, 924 cm^{-1}. HRMS-MALDI (m/z) [M + Na]$^+$: calcd for $C_{13}H_{23}NO_7S_2Na$, 392.08081; found, 392.08087. Anal. Calcd for $C_{13}H_{23}NO_7S_2$: C, 42.26; H, 6.27; N, 3.79; S, 17.36. Found: C, 42.04; H, 6.20; N, 3.72; S, 16.11.

ROP of EG_x-SS-Cys NCAs. All polymerizations were performed in a N_2-filled glovebox. To a solution of NCA in THF/DMF 1:1 v/v (50 mg/mL) was rapidly added a solution of hexamethyldisilazane (HMDS) in THF (0.1 mol/L). The reaction was stirred at room temperature, and polymerization progress was monitored by FTIR.

dx.doi.org/10.1021/ma501104s | Macromolecules 2014, 47, 4684–4689

Aliquots were sampled for GPC/LS analysis immediately upon polymerization completion. Sample solutions were removed from glovebox and precipitated into ethers. Solids were collected by centrifugation, washed another three times by ether and dried under reduced pressure to yield white to pale yellow solids (90−95% yield).

Poly-S-(2-(2-methoxyethoxy)ethyl)thio-L-cysteine (Poly-EG$_2$-SS-Cys), ***1c.*** ^{1}H NMR (400 MHz, DMSO-d_6): δ 8.35 (br s, 1H), 4.83−4.25 (br m, 1H), 3.73−3.57 (br m, 2H), 3.52 (br s, 2H), 3.44 (br m, 2H), 3.24 (s, 3H), 3.19−3.06 (br m, 2H), 3.04−2.77 (br m, 2H). FTIR (THF): 3282, 2921, 2875, 1660, 1526, 1406, 1353, 1288, 1242, 1101 cm^{-1}.

Poly-S-(2-(2-(2-methoxyethoxy)ethoxy)ethyl)thio-L-cysteine (Poly-EG$_3$-SS-Cys), ***2c.*** ^{1}H NMR (400 MHz, DMSO-d_6): δ 8.35 (br s, 8.35) 4.73−4.30 (br s, 1H), 3.74−3.58 (br m, 2H), 3.58−3.46 (br s, 6H), 3.46−3.38 (br m, 2H), 3.24 (s, 3H), 3.20−3.08 (br m, 2H), 2.89 (br m, 2H). FTIR (THF): 3281, 2918, 2872, 1697, 1631, 1521, 1458, 1408, 1352, 1298, 1242, 1200, 1109 cm^{-1}.

Poly-S-(2-(2-(2-(2-methoxyethoxy)ethoxy)ethoxy)ethyl)thio-L-cysteine (Poly-EG$_4$-SS-Cys), ***3c.*** ^{1}H NMR (400 MHz, DMSO-d_6): δ 8.35 (br s, 1H), 4.83−4.25 (br s, 1H), 3.73−3.57 (br m, 2H), 3.52 (br m, 10H), 3.44 (br m, 2H), 3.24 (s, 3H), 3.19−3.06 (br m, 2H), 3.04−2.77 (br m, 2H). FTIR (THF): 3279, 2920, 2876, 1697, 1632, 1518, 1456, 1406, 1352, 1296, 1246, 1198, 1109 cm^{-1}.

The mPEG-*b*-poly-EG$_4$-SS-Cys diblock was synthesized using mPEG$_{45}$-NH$_2$ (M_w = 2000) as macroinitiator. Typically, 54 mg of mPEG$_{45}$-NH$_2$ was dried in a 50 mL Schlenk flask at 100 °C in high vacuum for 5 h. Then, 5 mL of anhydrous THF was injected into the flask using a syringe followed by addition of 5 mL EG$_4$-SS-Cys NCA solution in THF (100 mg/mL). The mixture was stirred at 40 °C for 3 days and the consumption of NCA was confirmed by FTIR. The sample mixtures were precipitated into ether, collected by centrifugation, and dried under reduced pressure to give the product as a white solid with 75% yield.

Methoxypoly(ethylene glycol)-b-poly-S-(2-(2-(2-(2-methoxyethoxy)ethoxy)ethoxy)ethyl)thio-L-cysteine (mPEG-b-poly-EG$_4$-SS-Cys), ***3d.*** ^{1}H NMR (400 MHz, DMSO-d_6): δ 8.33 (br s, 1H), 4.57 (br s, 1H), 3.63 (br s, 2H), 3.51 (br s, 16H), 3.43 (br m, 3H), 3.24 (s, 3H), 3.14 (br m, 2H), 2.89 (br m, 2H). FTIR (THF): 3280, 2872, 1698, 1631, 1517, 1456, 1408, 1351, 1299, 1248, 1199, 1108 cm^{-1}.

RESULTS AND DISSCUSSION

OEGylated disulfide-containing L-cysteines (EG$_x$-SS-Cys, x = 2, 3, and 4) were prepared from OEG sulfenyl chlorides (EG$_x$-S-Cl) using modified reported procedures.[16] Then, three monomers were directly converted into the corresponding NCAs using triphosgene in THF at 50 °C. The obtained samples were first concentrated and followed by purification of flash column chromatography. The obtained three monomers were viscous oils.[17] From the ^{1}H NMR spectrum of **2b** in Figure 1a, the intensity ratio of cysteine methine protons at 4.77 ppm, methoxyl protons of OEG moiety at 3.23 ppm and two methylene protons adjacent to disulfide group at 3.18 and 2.91 ppm is close to 1:3:2:2, indicating quantitative OEGylation of cysteine. Also ^{13}C NMR spectrum, elemental analysis and MS confirm the successful preparation of three EG$_x$-SS-Cys NCA monomers.

ROP of EG$_x$-SS-Cys NCAs (**1b**, **2b**, and **3b**) was performed in mixture of THF/DMF (1:1 v/v) using HMDS as initiator.[18] The polymerization proceeded readily at ambient temperature to give the corresponding homopolypeptides, poly-EG$_x$-SS-Cys (**1c**, **2c**, and **3c**), with relative narrow polydispersity indices (PDIs) (see Table 1). Note that these NCAs can also be initiated using amines like alkyl amine and Et$_3$N, which unfortunately had less control over molecular weight and PDIs compared to HMDS. We also tried using Ni(0) as the initiator for ROP of **1b**, **2b**, and **3b** however without any success. Upon addition of Ni(COD)depe complex, the NCA solution turned from yellow to black gray within a few minutes, and subsequent FTIR characterization revealed no formation of peptide bonds and remaining of NCAs. A possible reason is that the sulfur could poison Ni(0) to deactivate the initiation process. In addition, Ni(0) as a strong reductive reagent may react with disulfide.[19] Note that the degrees of polymerization (DP) for **1c**, **2c**, and **3c** by HMDS were relatively low. We assumed the reason was due to low reactivity of **1b**, **2b**, and **3b**. Also, the insufficient purity of NCAs could be another possible reason. The obtained homopolypeptides were soluble in polar solvents such as DMSO, DMF, and methanol, but exhibited differences in THF, DCM and water. The results are summarized in Table S1. In particular, sample **1c** is insoluble in water while samples **2c** and **3c** have much better water solubility. The reason is that longer OEG chains offer better hydrophilicity.[20,21]

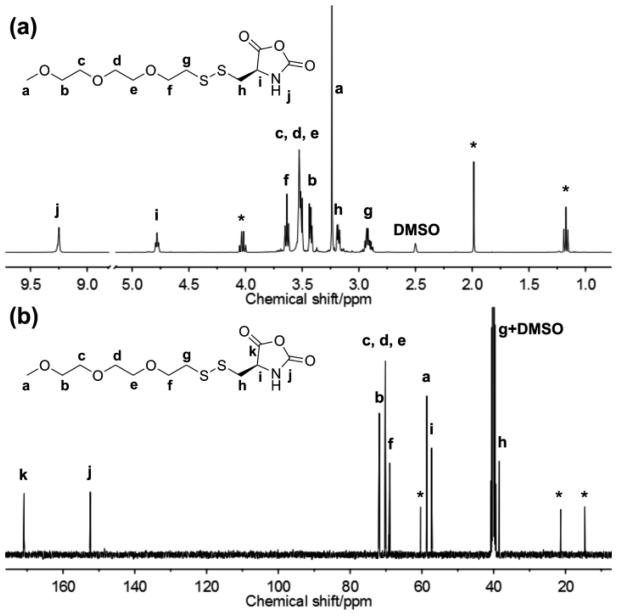

Figure 1. ^{1}H NMR (a) and ^{13}C NMR (b) spectra of EG$_3$-SS-Cys NCA (**2b**) in DMSO-d_6 (∗ indicates ethyl acetate residue).

We then studied the solution properties of samples **2c** and **3c** in water. As shown in Figure 2, both samples' solution became cloudy upon heating indicating expected thermal-responsive behaviors. Surprisingly, the cloudy solutions remained turbid after cooling the solution back to room temperature, which was in sharp contrast to conventional thermal-responsive polymers such as poly(*N*-isopropylacrylamide) (PNIPAM) or poly(oligoethylene glycol)methacrylates (POEGMAs), etc. Further keeping the solution in a quiescent state at 4 °C for 1 week did not turn it back to transparent. These results suggested that the temperature induced phase transition was apparently irreversible for at least 1 week. Figure 2b shows the solution transmittance as a function of temperature. For sample **2c**, the transmittance gradually decreased from 100% to 1% when temperature increased from 20 to 70 °C, while only recovered to 5% upon cooling. If we defined temperature with 50% transmittance as CP, the CP of sample **2c** is about 34 °C. In contrast, there was a sharp phase transition for sample **3c**. The transmittance decreased from 100% to 1% within narrow temperature window with corresponding CP being 45 °C. Again, cooling the solution only recovered 8% transmittance. Furthermore, these irreversible thermal-responsive behaviors

dx.doi.org/10.1021/ma501104s | *Macromolecules* 2014, 47, 4684−4689

Table 1. Molecular Parameters of poly-EG$_x$-SS-Cys

monomer[a]	[M]/[initiator][a]	M_n[b]	M_w/M_n[b]	DP[c]	yield/%[d]
EG_2-SS-Cys NCA	10	2600	1.30	11	90
EG_2-SS-Cys NCA	30	5700	1.13	24	82
EG_2-SS-Cys NCA	50	7900	1.25	30	80
EG_3-SS-Cys NCA	10	2500	1.25	9	87
EG_3-SS-Cys NCA	30	3800	1.17	13	80
EG_3-SS-Cys NCA	50	4500	1.13	16	85
EG_4-SS-Cys NCA	10	2500	1.19	8	78
EG_4-SS-Cys NCA	30	4700	1.21	15	82
EG_4-SS-Cys NCA	50	8300	1.23	26	75
EG_4-SS-Cys NCA*	50	11 700	1.10	30	75

[a]Number indicates equivalents of monomer per HMDS or mPEG-NH_2 (denoted with an asterisk (*)). [b]Molecular weight, polydispersity index and degree of polymerization as determined by GPC/LS. [c]Degree of polymerization as determined by ^{1}H NMR. [d]Total isolated yield of polypeptides.

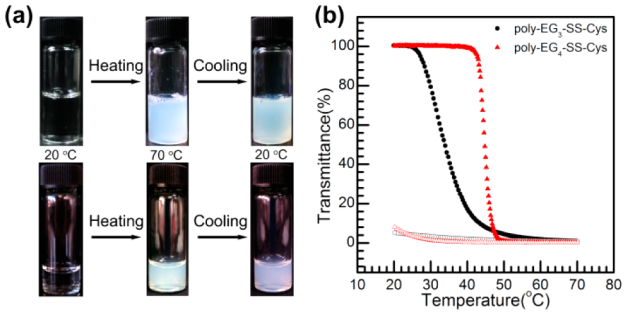

Figure 2. (a) Photos of temperature induced phase transition for samples poly-EG$_x$-SS-Cys (**2c**, top; **3c**, bottom) aqueous solutions at 2 mg/mL. (b) Transmittance as a function of temperature for aqueous solutions (2 mg/mL) of poly-EG$_x$-SS-Cys (**2c**, black; **3c**, red). Solid symbols: heating ramp. Open symbols: cooling ramp.

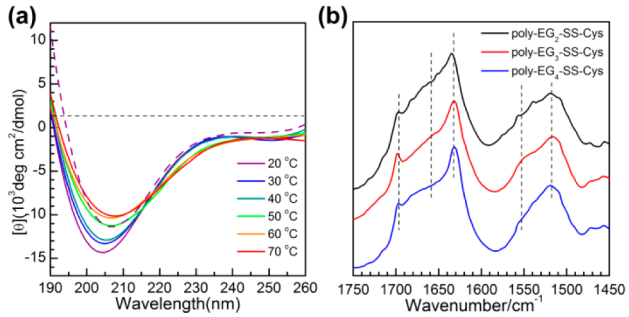

Figure 3. (a) CD spectra of **2c** aqueous solution (0.1 mg/mL) as a function of temperature (solid lines, heating ramp; dashed lines, cooling ramp); (b) FTIR spectra of poly-EG$_x$-SS-Cys (from top to bottom: **1c**, **2c**, and **3c**).

were observed to be independent of heating/cooling rates, and corresponding CPs increased with decrease of concentrations (see Figures S1 and S2).

For traditional thermal-responsive polymers such as PNIPAM and POEGMAs, the responsive mechanism mostly arose from the delicate hydrophilic/hydrophobic balances of polymer subunits. For those polymers containing OEG unit, the reversible dehydration/rehydration upon heating/cooling was the main reason for their thermal-responsive properties. Meanwhile, for polypeptides, the situation became more complicated. Besides the chemical structures of subunits and compositions, polypeptides have inherent secondary structures that are also critical factors to obtain thermal-response properties because the nature of secondary structure determines the characteristic of hydrogen bonding interactions, i.e., intramolecular interactions vs intermolecular interactions.[22,23] Considering these, we then investigated the possible conformation changes for samples **2c** and **3c** in course of heating/cooling procedures using circular dichroism (CD) spectroscopy. The data are shown in Figure 3a and Figure S3. CD spectra indicated that both samples mainly adopted random coil conformation. The conformation of **2c** at 20 °C was composed of about 14% helix, 21% β-sheet, 20% turns and 45% random coil; and for **3c**, there were 17% helix, 27% β-sheet, 21% turns and 35% random coil. Heating the solutions above their CPs did not alter the conformation significantly (Table S2). The conformation of poly-EG$_x$-SS-Cys in solid state was characterized using FTIR (Figure 3b). All three samples showed strong absorption bands at 1631 and 1518 cm^{-1} and a shoulder peak at 1698 cm^{-1}, indicating predominant antiparallel β-sheet conformation.[24,25] Absorption bands with low intensity around 1650 and 1550 cm^{-1} were also observed indicating existence of α-helix or random coil. The conformation characteristic revealed the origins of their distinct solubility in water. They all adopted β-sheet as major conformation in solid state. Once dispersed in water, only long enough OEG side-chain can offer sufficient hydrophilicity to break the intermolecular hydrogen bonding and ensure dispersing or dissolution of samples. As discussed later, sample **2c** was found to form nanoscopic aggregates in water as revealed by light scattering while sample **3c** was full soluble in water provided no heating history.

Another question to understand is the temperature induced irreversible phase transition. We need to figure out whether any chemical reactions occurred or not. Dynamic light scattering (DLS) was applied to track the phase transition during heating procedure (Figure 4). Here the *Z*-average radii and derivative count rate (DCR) were used to represent aggregate sizes and scattering light intensity, respectively. DLS measurements indicated that sample **2c** formed aggregates with average sizes about 60 nm at room temperature. There was a slight increase of aggregates size from 66 to 78 nm when the solution was heated above CP. These results indicated that sample **2c** might already form loosely associated aggregates before heating, which suggested relative lower solubility compared to sample **3c**. On the other hand, an abrupt increase of DCR was observed at 35 °C, which verified the LCST behaviors and also displayed consistent CP. In contrast, DLS measurements revealed minimal aggregates, which suggested fully dissolution for sample **3c** at room temperature. Negligible DCR below phase transition temperature further support this conclusion.

dx.doi.org/10.1021/ma501104s | *Macromolecules* 2014, 47, 4684−4689

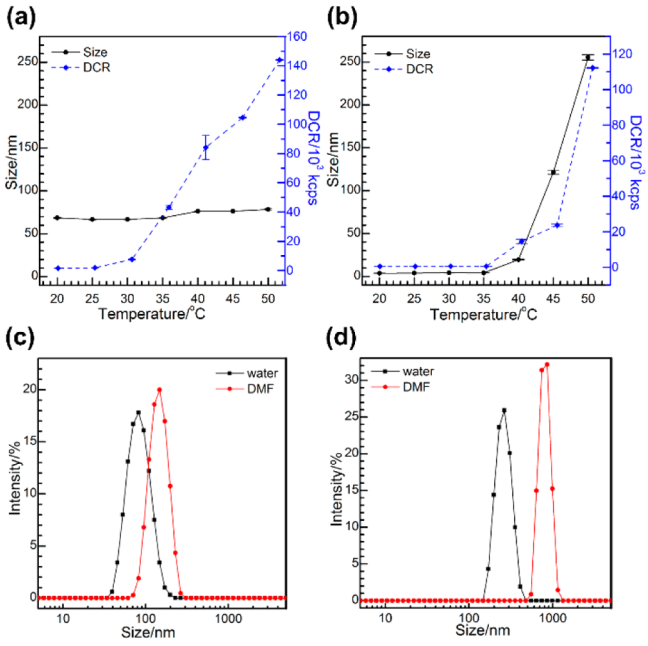

Figure 4. DLS data of poly-EG$_3$-SS-Cys (a, c) and poly-EG$_4$-SS-Cys (b, d). (a, b) Size (average radius, solid circles) and intensity (solid diamonds) changes of aqueous solutions (2 mg/mL) as a function of temperature. (c, d) Size distributions at 50 °C before and after 10-fold dilution with DMF.

Upon heating the solution, a turning point for both aggregates size and DCR appeared at 40 °C, which agreed well with CP determined by turbidimetry. It was known OEGylated polyglutamates and related copolymers can display conformation specific thermal-responsive properties and self-assembly behaviors, respectively.[26−28] On the other hand, some OEGylated polypeptides showed dual thermal- and oxidation responsive.[10] Apparently, things became more complicated for these disulfide containing poly(L-cysteine)s. As we noted already, cooling the cloudy solution back to 4 °C, which was well below the CP, did not recover the dissolution for both samples **2c** and **3c**. These results indicated not just simple physical aggregation but possible chemical linkage occurred during heating. Considering the chemical structures of poly-EG$_x$-SS-Cys, we hypothesized there may be intermolecular disulfide bonds formation in these polypeptides, which resulted in chemical cross-linking among polypeptides.

To examine our hypothesis, we added DMF, which was a good solvent for poly-EG$_x$-SS-Cys, to the sample solution after phase separation. If the temperature induced aggregation was caused only by physical interactions, addition of DMF will disrupt the interaction and disintegrate the aggregates. Otherwise, addition of DMF will only swell the aggregates. For samples **2c** and **3c**, we diluted the already heated solution with DMF, but both solutions maintained the cloudiness. Then, we tried adding 0.1, 1 and 10-fold DMF, only the last one showed distinct size changes because of swelling. DLS characterization revealed that the average aggregates sizes increased from 78 to 127 nm for sample **2c** and from 255 to 865 nm for sample **3c**, respectively. These results confirmed the existence of chemical cross-linking in the aggregates of **2c** and **3c**, which was most likely caused by the intermolecular disulfide exchange reactions. Note that such cross-linking could also occur at room temperature, and heating only accelerates the reaction. The reason was that the local disulfide bonds concentration was substantially increased above CP, which accordingly facilitated the cross-linking reactions. A freshly prepared **3c** solution could stay clear for more than 1 week at room temperature without heating, but became cloudy gradually over time and cannot turn back transparent even at 4 °C for extended time. Considering the majority of unsymmetrical disulfide bonds and negligible free thiol groups in these polypeptide solutions, we propose a dominant disulfide−disulfide interchange mechanism rather than the conventional thiol−disulfide exchange.[29] It was generally known that homolysis of disulfide bond into thiyl radicals required quite high energy like heating to above 170 °C or under UV radiation.[30,31] Therefore, it is most likely due to ionic process generating thiolates in this case.

It is worth noting that such heating induced disulfide interchange could be useful for constructing novel stimuli responsive biomaterials, for example chemical cross-linking micelles, vesicles and hydrogels for biomedical applications. It becomes easy to generate intermolecular disulfide bonds for cross-link by simply heating instead of DTT treating.[32−34] Based on these irreversible thermal-responsive properties of disulfide bond containing poly(L-cysteine), we considered using them to construct a thermal gel. Moreover, the heating induced chemical cross-linking of disulfide bonds can be applied as reactive sites for further reduction, providing external stimuli response. We then synthesized a mPEG$_{45}$-*b*-poly(L-EG$_4$-SS-Cys)$_{24}$ diblock copolymer (**3d**) via ROP of **3b** using mPEG-NH$_2$ as macromolecular initiator. The corresponding diblock was characterized using NMR and GPC (Scheme S1 and Table 1). FTIR and CD spectra revealed that the peptide block adopted a predominant β-sheet conformation as evident from the amide I band at 1631 cm^{-1}and the minimum at 224 nm in the CD spectrum (Figure S4, Table S2). Heating the dilute solution of **3d** also resulted in irreversible LCST behavior determined by turbidimetry (Figure S5). While for the aqueous solutions of sample **3d** with concentrations above 2 wt %, thermal induced gelation was observed upon heated to 50 °C, and there was no gel−sol transition upon cooling to 20 °C (Figure 5a). The hydrogel strength was characterized by

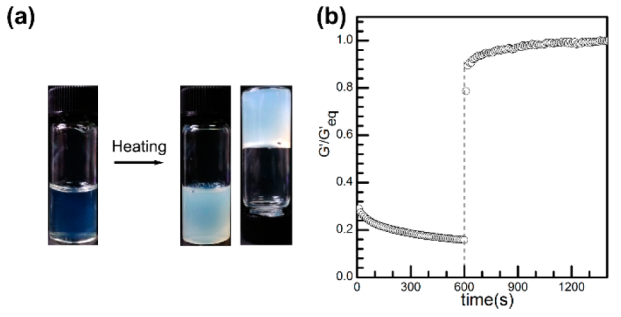

Figure 5. (a) Photo of thermal-induced sol−gel transition for aqueous solution of sample **3d** at 2 wt %. (b) G'/G'_{eq} as a function of time for sample **3d** hydrogel, sheared at ω = 6 rad/s, γ_0 = 50 for 600 s before switching to γ_0 = 0.4. For comparison, G' was normalized to the equilibrium value (G'_{eq}).

rheology (Figure 5b and Figure S6), and the storage modulus and loss modulus were ∼100 and 2 Pa, respectively, indicating a soft hydrogel formation. Moreover, the hydrogel showed rapid recovery after a shear-thinning process. Under large amplitude strain oscillations the hydrogel underwent a partial gel−sol transition with strength decreased to 18%. Then upon removal

dx.doi.org/10.1021/ma501104s | *Macromolecules* 2014, 47, 4684−4689

of shearing, it recovered to gel status of 90% strength within 6 s, and regained 100% of original strength within 10 min. Considering the thermal induced disulfide bonds exchange in homopolypeptides, it was probably in the same situation for the diblock copolymer. During thermal hydrogelation process, intermolecular disulfide bond formed, and physical cross-linking hydrogel converted to partially chemical cross-linking status, resulting in incomplete shear-thinning under large strain. Upon removal of shearing hydrogen bonding reformed and the hydrogel strength recovered. For the mechanism of hydrogel formation and rapid recovery properties, we believed owing to the predominant β-sheet conformation of peptide block, and this made the diblock copolymer hydrogel to show great potential as reduction-responsive injectable hydrogel in biomedical applications.

CONCLUSIONS

In summary, we developed a new method to prepare OEGylated disulfide bond-containing poly(L-cysteine)s via ROP of NCAs. These homopolypeptide containing three and four ethylene glycol units displayed thermal-responsive properties because of the OEG moieties, but the temperature induced phase transition was irreversible due most likely to intermolecular disulfide bond formation upon heating. The $mPEG_{45}$-*b*-poly(L-EG_4-SS-Cys)$_{24}$ diblock can undergo an irreversible thermal hydrogelation, and the hydrogel displayed partially shear-thinning and rapid recovery properties. These new stimuli-responsive polypeptides are promising material to construct multi-responsive polypeptide based hydrogels or nanogels for smart delivery systems.

ASSOCIATED CONTENT

Supporting Information

Solubility and structure compositions, synthesis scheme, phase transition plots, photos of the phase transition, storage and loss moduli, additional CD, UV, and NMR spectra, and GPC results. This material is available free of charge via the Internet at http://pubs.acs.org.

AUTHOR INFORMATION

Corresponding Authors

* E-mail: fuwenxin@iccas.ac.cn (W.F.).
* E-mail: zbli@iccas.ac.cn (Z.L.).

Notes

The authors declare no competing financial interest.

ACKNOWLEDGMENTS

The authors appreciate financial support from the NSFC Funding for Distinguished Young Scholar (51225306).

REFERENCES

(1) Góngora-Benítez, M.; Tulla-Puche, J.; Albericio, F. *Chem. Rev.* **2013**, *114*, 901−926.
(2) Paulsen, C. E.; Carroll, K. S. *Chem. Rev.* **2013**, *113*, 4633−4679.
(3) Sevier, C. S.; Kaiser, C. A. *Nat. Rev. Mol. Cell Biol.* **2002**, *3*, 836−847.
(4) Gilbert, H. F., Molecular and Cellular Aspects of Thiol−Disulfide Exchange. In *Adv. Enzymol. Relat. Areas Mol. Biol.*; John Wiley & Sons, Inc.: New York, 2006; pp 69−172.
(5) Berger, A.; Noguchi, J.; Katchalski, E. *J. Am. Chem. Soc.* **1956**, *78*, 4483−4488.
(6) Kramer, J. R.; Deming, T. J. *J. Am. Chem. Soc.* **2012**, *134*, 4112−4115.
(7) Zhou, J.; Chen, P.; Deng, C.; Meng, F.; Cheng, R.; Zhong, Z. *Macromolecules* **2013**, *46*, 6723−6730.
(8) Das, S.; Kar, M.; Gupta, S. S. *Polym. Chem.* **2013**, *4*, 4087−4091.
(9) Liu, G.; Dong, C. M. *Biomacromolecules* **2012**, *13*, 1573−1583.
(10) Fu, X.; Shen, Y.; Fu, W.; Li, Z. *Macromolecules* **2013**, *46*, 3753−3760.
(11) Fu, X.; Ma, Y.; Shen, Y.; Fu, W.; Li, Z. *Biomacromolecules* **2014**, *15*, 1055−1061.
(12) Meng, F.; Hennink, W. E.; Zhong, Z. *Biomaterials* **2009**, *30*, 2180−2198.
(13) Whitmore, L.; Wallace, B. A. *Nucleic Acids Res.* **2004**, *32*, W668−W673.
(14) Whitmore, L.; Wallace, B. A. *Biopolymers* **2008**, *89*, 392−400.
(15) Snow, A. W.; Foos, E. E. *Synthesis-Stuttgart* **2003**, 509−512.
(16) Rietman, B. H.; Peters, R. F. R.; Tesser, G. I. *Synth. Commun.* **1994**, *24*, 1323−1332.
(17) Kramer, J. R.; Deming, T. J. *Biomacromolecules* **2010**, *11*, 3668−3672.
(18) Lu, H.; Cheng, J. *J. Am. Chem. Soc.* **2007**, *129*, 14114−14115.
(19) Deming, T. J. *Nature* **1997**, *390*, 386−389.
(20) Hu, Z.; Cai, T.; Chi, C. *Soft Matter* **2010**, *6*, 2115−2123.
(21) Lutz, J. F. *Adv. Mater.* **2011**, *23*, 2237−2243.
(22) Hwang, J. Y.; Deming, T. J. *Biomacromolecules* **2001**, *2*, 17−21.
(23) Yu, M.; Nowak, A. P.; Deming, T. J.; Pochan, D. J. *J. Am. Chem. Soc.* **1999**, *121*, 12210−12211.
(24) Elliott, A. *Proc. R. Soc. A* **1954**, *221*, 104−114.
(25) Haris, P. I.; Chapman, D. *Biopolymers* **1995**, *37*, 251−263.
(26) Chen, C.; Wang, Z.; Li, Z. *Biomacromolecules* **2011**, *12*, 2859−2863.
(27) Zhang, S.; Chen, C. *Chin. J. Polym. Sci.* **2013**, *31*, 201−210.
(28) Shen, J.; Chen, C.; Fu, W.; Shi, L.; Li, Z. *Langmuir* **2013**, *29*, 6271−6278.
(29) Parker, A. J.; Kharasch, N. *Chem. Rev.* **1959**, *59*, 583−628.
(30) Koval', I. *Russ. Chem. Rev.* **1994**, *63*, 735−750.
(31) Dénès, F.; Pichowicz, M.; Povie, G.; Renaud, P. *Chem. Rev.* **2014**, *114*, 2587−2693.
(32) Ryu, J.-H.; Bickerton, S.; Zhuang, J.; Thayumanavan, S. *Biomacromolecules* **2012**, *13*, 1515−1522.
(33) Zhuang, J.; Chacko, R.; Amado Torres, D. F.; Wang, H.; Thayumanavan, S. *ACS Macro Lett.* **2013**, *3*, 1−5.
(34) Ryu, J.-H.; Chacko, R. T.; Jiwpanich, S.; Bickerton, S.; Babu, R. P.; Thayumanavan, S. *J. Am. Chem. Soc.* **2010**, *132*, 17227−17235.